Development of a selective ammonia YSZ-based sensor and modeling of its response

Gita Nematbakhsh Abkenar, Mathilde Rieu, Philippe Breuil, Jean-Paul Viricelle

Development of a selective ammonia YSZ-based sensor and modeling of its response

Gita Nematbakhsh Abkenar, Mathilde Rieu*, Philippe Breuil, Jean-Paul Viricelle

Mines Saint-Etienne, Univ Lyon, CNRS, UMR 5307 LGF, Centre SPIN, F-42023, Saint-Etienne, France.

***** Corresponding author: M. Rieu. E-mail: rieu@emse.fr

Abstract: In the present study, Au-V_2O_5 sensing material was tested as a sensing electrode for developing mixed-potential ammonia gas sensors. The results of gas sensing measurements indicated selective responses to NH_3 while this selectivity was highly dependent on the temperature. Different V_2O_5 contents were tested in the sensing electrode. The results showed that by increasing V_2O_5 content from 15 wt.% to 50 wt.%, selective ammonia sensors could be achieved at 550 °C. The selectivity of Au-50%V_2O_5 sensor was also confirmed in gas mixtures of CO, NH_3, NO, and NO_2 gases. Modeling of the sensor responses in the ammonia concentration range 2-40 ppm at four oxygen concentrations was performed based on mixed-potential theory. Nernst and Butler-Volmer equations with an electron transfer assumption were used for data modeling.

Keywords: Mixed-potential gas sensor, Ammonia, Sensing electrode, V_2O_5, Response modeling.

Highlights

High temperature ammonia gas sensors were studied.

Au-V_2O_5 sensing electrode was sensitive and selective to NH_3.

Gas sensor responses were modeled according to mixed potential theory.

1. Introduction

Selective catalyst reduction (SCR) system using ammonia gas as a reductant is one of the most reliable ways to reduce NO_x emissions from diesel engine vehicles and trucks. To optimize the conversion rates of NO_x and to prevent inducing excessive NH_3 to the air, an ammonia sensor is required to control the SCR system [1]. There are wide ranges of studies in the literature to find a robust, sensitive, low cost and selective ammonia sensor working at high temperatures.

One of the most promising solid-state ammonia sensors suitable for harsh environments is mixed-potential type sensors with yttria-stabilized zirconia (YSZ) electrolyte [2-4]. The main advantages of these mixed-potential type gas sensors that distinguish them from other types of sensors, are higher stability and reproducibility, wide flexibility for targeting gas species by changing the composition of the electrodes operating under open circuit or biased mode, and the ability to detect changes in gas content on timescales of milliseconds [5]. Indeed, these sensors have special features such as high-temperature operation, excellent sensing performance, and high chemical and mechanical stability [6]. They have also been studied extensively due to their fast response, high sensitivity, and long-term stable results [3, 4].

So far, numerous studies have been performed to find a sensitive and selective ammonia sensor at high temperatures. Different approaches have been suggested to achieve an effective ammonia sensor by modifying electrolyte [7, 8], reference electrode [3,9] or sensing electrode [9-16].

Indeed, in these sensors, choosing a suitable material as a sensing electrode is very important for developing sensitive and selective sensors. A high electro-catalytic activity, as well as catalytic selectivity, are imperative for the sensing element of these sensors, especially in planar configuration. Among them, vanadium based sensing electrodes looks very promising. For example, Wang et al. in 2006 [9] published a patent (from Delphi Inc.) in which they reported the results of nineteen different sensors with various vanadium based electrode materials. After testing different materials, they found $BiVO_4$ as the most appropriate material for a selective ammonia sensor. Liu et al. in 2015 [16] developed a sensor using stabilized zirconia (YSZ) and sensing electrode (SE) of $Ni_3V_2O_8$ oxide. They showed that $Ni_3V_2O_8$ calcined at 1000 °C exhibited the largest sensitivity in an NH_3 concentration range of 50-500 ppm at 650 °C. Wang et al. in 2016 [12] used V_2O_5–WO_3–TiO_2 (VWT) material to get an ammonia selective electrode. The sensing electrode was consisted of Pt covered with a porous VWT catalyst layer.

In addition, vanadium dioxide (V_2O_5) is also well-known as sensitive material to ammonia even at ppb levels [12, 17].

Taking into account our past results with Pt/YSZ/Au configuration for NOx sensors [18-20] and literature results dealing with NH_3 sensors, especially based on V_2O_5 material, the objective of the present study is to developed sensitive and selective NH_3 sensors, using Au-V_2O_5 material as sensing electrode. For this, three mass percentages of V_2O_5 to Au (15, 30, and 50 wt.%) are used. The results of these sensors to different interfering gases such as CO, NO_2, NO, H_2, and hydrocarbons are studied. In addition, sensor responses to different O_2 and NH_3 concentrations are investigated. Finally, mixed potential theory based on Butler-Volmer equation is used to model the obtained results.

2. Experimental

The fabrication of sensors was performed by a screen-printing method using R-23 Meteor 23 semi-automatic screen-printer. Commercially available Pt (ESL 5545) and Au (ESL 8880-H) inks were used while YSZ (TZ-8YS) and V_2O_5 (Sigma-Aldrich) homemade inks were elaborated using commercial powders. For preparing homemade inks, a binder (ESL V400A) and an organic solvent (ESL 404) were added to commercial powders. For Au-V_2O_5 sensing electrodes, a mixture of Au commercial ink and V_2O_5 home-made ink was prepared with 15, 30 and 50 wt.% of V_2O_5.

The sensors were developed in planar configuration on alumina substrates as supports. A YSZ electrolyte layer was first deposited on the substrate following by 2 hours sintering at 1380 °C. The reference (RE: Pt) and sensing electrodes (SE: Au or Au-V_2O_5) were then printed on the YSZ layer. The sintering temperatures for Pt reference electrode and Au-V_2O_5 sensing electrode were 850 °C and 600 °C during 1 hour respectively. In order to provide the high working temperature of sensors, a heating element in the form of a platinum resistor was printed on the opposite side of the alumina substrate, facing the YSZ electrolyte. Fig. 1 shows the sensing and heating sides of a final sensor with different elements. Although Pt electrode is not in a reference chamber as the sensor is in planar configuration, we keep the name “reference electrode (RE)” as it has been shown that Pt behaves like a reference in such single chamber, in regards of other oxide based electrodes designed as sensing electrodes (SE) [21].

To identify the sensors with different sensing elements, the mass percentage of V_2O_5 is indicated in their name. Sensors with 15 wt.% V_2O_5 are named as Au-15%V_2O_5, with the same labeling for 30 wt.% V_2O_5 (Au-30%V_2O_5), and 50 wt.% V_2O_5 (Au-50%V_2O_5).

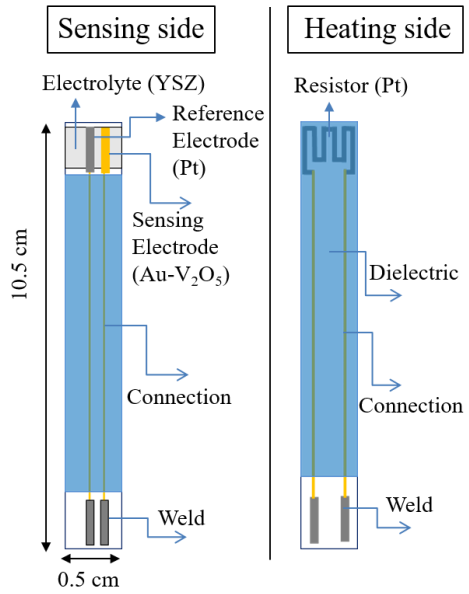

Fig. 1 Scheme of fabricated sensor by screen-printing technology.

A test bench was used to study the responses of two sensors working simultaneously in separate cells, thus allowing to check the signal reproducibility. A schematic of the experimental test bench is shown in Fig. 2. The various studied gases were conditioned in separated cylinders and their flow rates were monitored by mass flow regulators. The total flow rate was fixed at 60 l/h, corresponding to 30 l/h per cell. An humidifier allowed to generate and control water vapor in the gas flow. Gases first arrived in a mixing chamber before being sent to the two cells, which each contained one sensor. An FTIR gas analyzer (Gasmet DX 4015) was used to analyze the gas leaving sensor cells.

Sensors responses to different gases such as CO, NH_3, NO_2, NO, H_2 and C_xH_y were studied. The hydrocarbon gas (C_xH_y) used in this study was composed of 56 mol.% propene (C_3H_6), 28 mol.% n-butane (n-C_4H_{10}) and 16 mol.% methane (CH_4). The base gas was composed of 2, 5, 12 or 16.4 mol.% O_2 balanced with N_2 with 1.5 vol.% absolute humidity. The sensor signal (ΔV_{RE}^0) is the potential difference between the reference electrode and the sensing electrode (ΔV_{RE}^0= V_{RE} -V_{SE}). Then, the response to a target gas is defined as the difference of the sensor signal in presence of this gas minus the sensor signal under base gas with the same oxygen content (response = $\Delta V_{RE,gas}^0 - \Delta V_{RE,basegas}^0$).

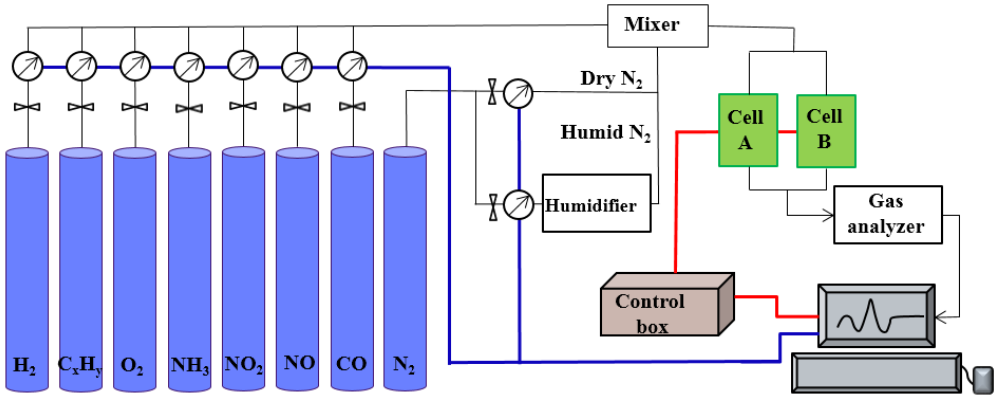

Fig. 2 Schematic of experimental test bench.

3. Results and discussions

3.1 Comparison between Au and Au-15%V_2O_5 sensing electrodes: influence of operating temperature

Sensors with Au and Au-15%V_2O_5 sensing electrodes were exposed successively to 100 ppm CO, NO_2, NO, and 20 ppm of NH_3 at different working temperatures in the range 450-600°C. The base gas in this experiment was composed of 12 mol.% O_2 balanced with N_2 and 1.5 vol.% absolute humidity. First, to emphasize the interest of V_2O_5 based electrodes, responses of Pt/YSZ/Au-15%V_2O_5 sensors were compared to the ones of a Pt/YSZ/Au sensors already reported for NOx detection in our previous studies [19- 20]. With our definition of sensor signal (ΔV_{RE}^0= V_{RE} -V_{SE}) and response, a typical behavior of such Pt/YSZ/Au sensors is a positive response to reducing gases (CO, NO and NH_3), and a negative one to oxidants ones like NO_2. Figure 3 showing the signal of an Au-15%V_2O_5 based sensor confirms that the substitution of Au by Au-15%V_2O_5 as sensing electrode does not modify qualitatively the behavior.

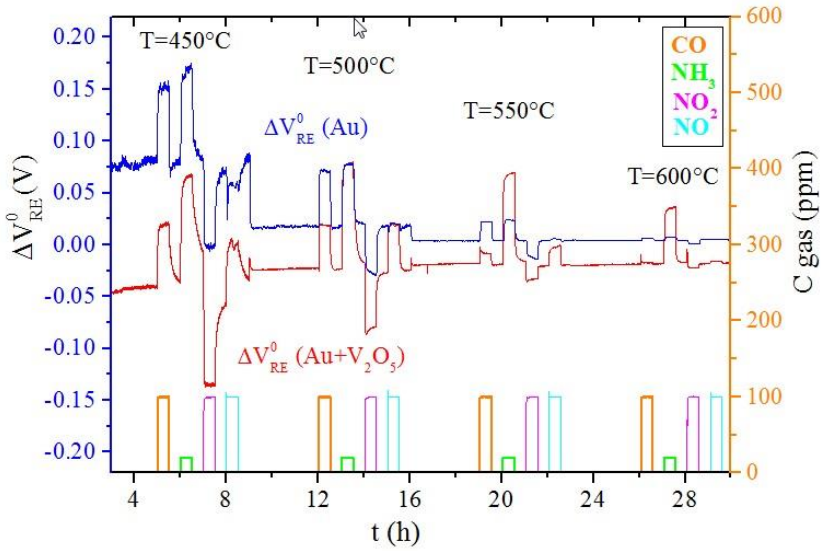

Fig. 3 Signals of sensors with Au (in blue) and Au-15%V_2O_5 (in red) sensing electrodes for 100 ppm CO, NO_2, NO and 20 ppm of NH_3 at 450, 500, 550, and 600 °C, in the base gas with 12 mol.% O_2.

By comparing quantitatively responses of both types of sensors (Table 1), it can be observed that responses related to Au electrode decrease considerably by increasing temperature from 450°C (absolute value in the range 14-87 mV) up to 600°C (absolute value lower than 3 mV). Regarding Au-15%V_2O_5 device, responses to CO, NO_2 and NO also decrease in a similar way when the temperature is increased. However, NH_3 response is quite less affected: its response decreases from 91mV (450°C) down to 66mV at 600°C, which remains significant in regards of the one of other gases. Hence, a selective ammonia sensor is obtained when increasing the temperature as the cross-sensitivity to other interfering gases, such as CO, NO_2 and NO, is strongly reduced at 600°C, as seen in figure 3.

Table 1 Comparison of Au and Au-15%V_2O_5 electrodes in sensor responses to pulses of CO (100 ppm), NH_3 (20 ppm), NO_2 (100 ppm) and NO (100 ppm) in base gas at different temperatures.

Temperature (°C)	Sensor	CO response (mV)	NH_3 response (mV)	NO_2 response (mV)	NO response (mV)
450	Au	72	87	-82	14
	Au-15%V_2O_5	**51**	**91**	**-65**	**52**
500	Au	53	58	-38	7
	Au-15%V_2O_5	**25**	**91**	**-27**	**29**
550	Au	18	20	-15	2
	Au-15%V_2O_5	**19**	**84**	**-32**	**21**
600	Au	2	3	-3	0
	Au-15%V_2O_5	**2**	**66**	**-5**	**3**

3.2 Effect of V_2O_5 content in Au-V_2O_5 sensing electrode

In addition to 15 wt.% of V_2O_5, two other mass percentages of V_2O_5 were tested in the sensing electrode (30 wt.% and 50 wt.% of V_2O_5). The different sensors (Au-15%V_2O_5, Au-30%V_2O_5 and Au-50%V_2O_5) were exposed to 100 ppm CO, NO_2, NO, and 20 ppm of NH_3 at four temperatures of 450, 500, 550 and 600 °C. The base gas was again composed of 12 mol.% O_2 balanced with N_2 and 1.5 vol.% absolute humidity. Gas responses of these sensors (absolute value for NO_2) were compared with each other at the four temperatures in Fig. 4. The results show that the gas responses for all sensors decrease by increasing the temperature (as observed before for Au-15%V_2O_5). Sensors respond significantly to all gases at 450 °C and 500 °C. By increasing the temperature up to 550 °C, the selectivity of 30%V_2O_5 and 50%V_2O_5 sensors for NH_3 detection is largely increased, while 15%V_2O_5 sensors still show responses to CO, NO_2 and NO at this temperature. Finally, all sensors show selective responses toward ammonia at 600 °C.

One of the main challenges of these sensors is long-term stability. Since the melting point of V_2O_5 is 680 °C [22] (650 °C in some studies [23]), there is a high possibility that an operating

temperature of 600°C for a long period could cause damage of Au-V_2O_5 sensing electrode. Indeed, test conducted at 600°C during 48 hours have confirmed a strong degradation of the sensing electrode, contrary to observations made after similar experiments at 550°C showing neither electrode degradation, nor sensor signal alteration. Therefore, a temperature of 550°C is a good compromise between long-term stability and NH_3 selectivity.

At 550°C, since 50%V_2O_5 based sensors show a slightly improved selectivity compared to 30%V_2O_5 ones, especially regarding CO interference, Au-50%V_2O_5 sensor was selected for the rest of this study.

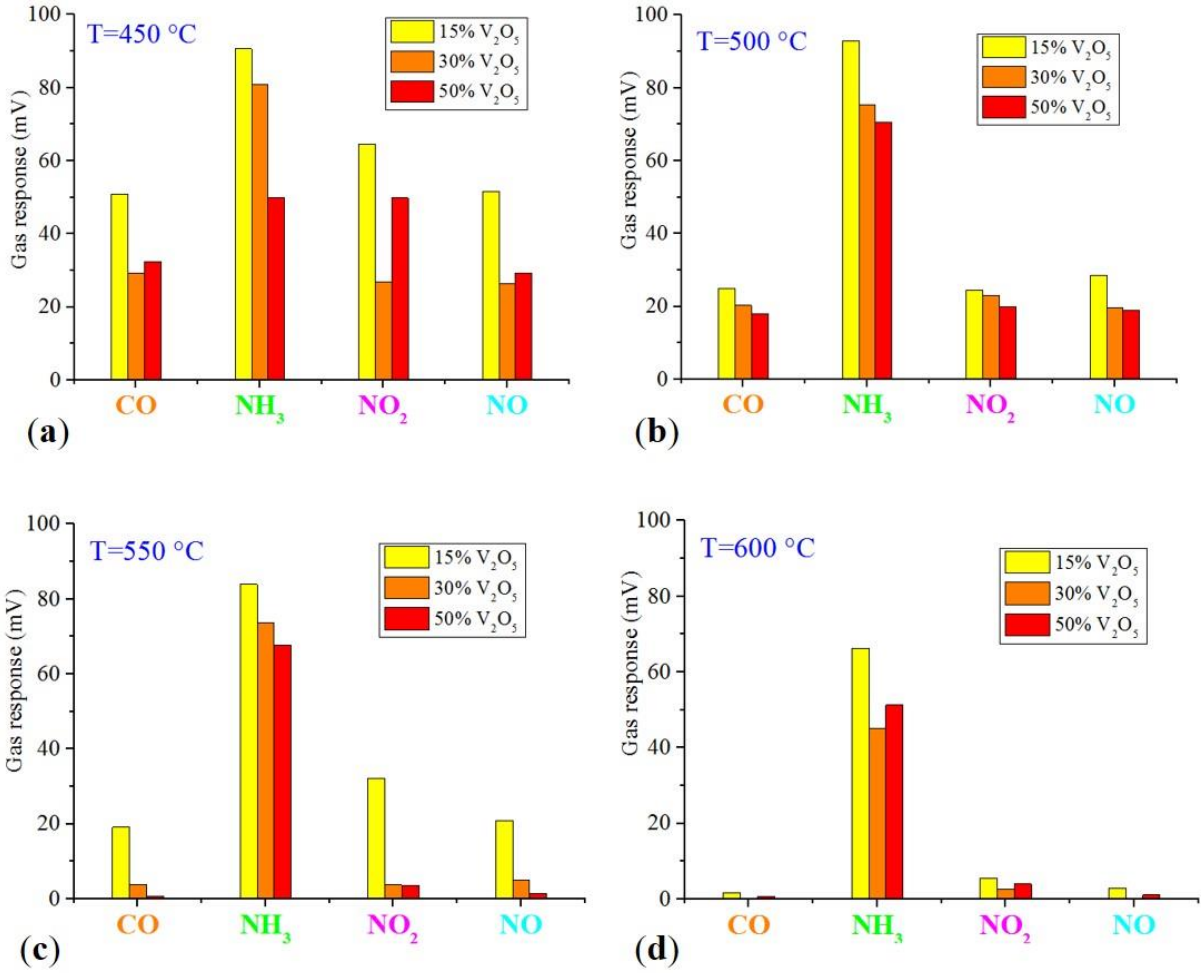

Fig. 4 Gas sensor responses (absolute value for NO_2) of Au-V_2O_5 based sensors with three mass percentages of 15%, 30% and 50% of V_2O_5 at (a) 450 °C, (b) 500°C, (c) 550 °C, and (d) 600°C.

3.3 Morphology of Au-50%V_2O_5 electrode on YSZ electrolyte

The morphology of the selected Au-50%V_2O_5 sensing electrode was characterized by Scanning Electron Microscopy (SEM, ZEISS SUP RA-55 VP). Cross-section micrograph is shown in Fig. 5. It can be seen that Au particles (white color) are well dispersed in the whole porous sensing electrode. Although the mass percentage of V_2O_5 and Au is 50-50 in this electrode, Au particles quantity seems to be lower than that of V_2O_5. In fact, 50 wt.% of V_2O_5 corresponds to 85 vol.% V_2O_5, due to the high density of gold compared to V_2O_5 (19.32 g.cm^{-3} for Au compared to 3.36 g.cm^{-3} for V_2O_5).

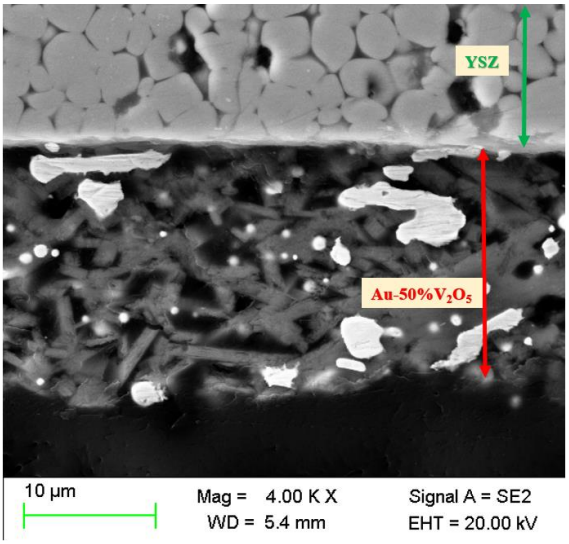

Fig. 5 Cross-section SEM micrograph of Au-50%V_2O_5 electrode on YSZ electrolyte.

3.4 Interference of H_2 and C_xH_y gases

In prior tests, four gases CO, NH_3, NO_2, and NO were tested to study the selectivity of the sensors. However, the sensor may be affected by other interfering gases. Hydrocarbons (HC) are among the most important species that may cause interference for NH_3 sensors in car exhaust. Apart from hydrocarbons, almost all diesel-type vehicles emit marginal amounts of hydrogen (around 0.1 mg/km). In some studies, hydrogen is reported as an interfering gas to the results of ammonia sensors [8]. Therefore, cross-sensitivity with these gases is also an important issue. To ensure the selectivity, Au-50%V_2O_5 sensors were tested with 100 ppm hydrocarbon (56 mol.% C_3H_6, 28 mol.% n-C_4H_{10}, 16 mol.% CH_4) and 20 ppm of H_2 at 550 °C.

The base gas in this experiment was also composed of 12 mol.% O_2 balanced with N_2 and 1.5 vol.% absolute humidity.

Fig 6. shows the response of a Au-50%V_2O_5 sensor to 100 ppm of CO, 20 ppm of NH_3, 100ppm of NO, 100ppm of NO_2, 100 ppm of C_xHy (2 times) and 20 ppm of H_2 (4 times). The results in Fig. 6 clearly show that sensors display no responses to CO, NO and NO_2 as previously seen and neither to hydrocarbons nor to hydrogen at 550 °C.

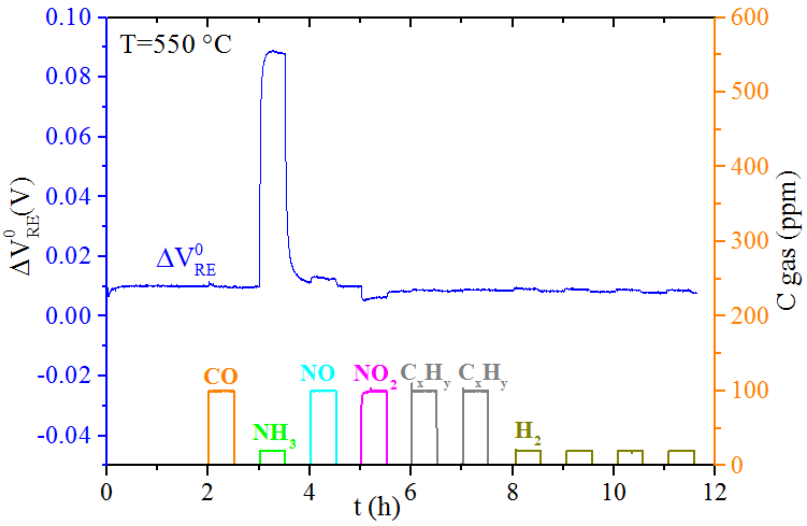

Fig. 6 Au-50%V_2O_5 sensor signal for 100 ppm of CO, 20 ppm of NH_3, 100 ppm of NO, 100 ppm of NO_2, 100 ppm of C_xH_y (2 times), and 20 ppm of H_2 (4 times) at 550 °C.

3.5 Au-50%V_2O_5 sensors responses in gas mixtures

Moreover, in previous tests, the sensing performances were studied with individual gases. However, in a real environment of gas exhaust, the pollutant gases exist altogether, which might disturb the responses of sensors to each gas. For this reason, sensors responses in gas mixtures were studied. To understand if the sensors responses were coherent with the gas existing in the mixture, a gas analyzer instrument (Gasmet DX 4015 FTIR analyzer) was used to monitor the gas composition at the exit of sensors cells. The sensor responses in different gas mixtures (set points of 10 ppm NH_3, 30 ppm NO_2 and 50 ppm CO and NO) are shown in Fig. 7 (with 12 mol.% O_2 balanced with N_2 and 1.5 vol.% absolute humidity as base gas). Fig. 7 also shows results of gas analyses and gas concentration set point.

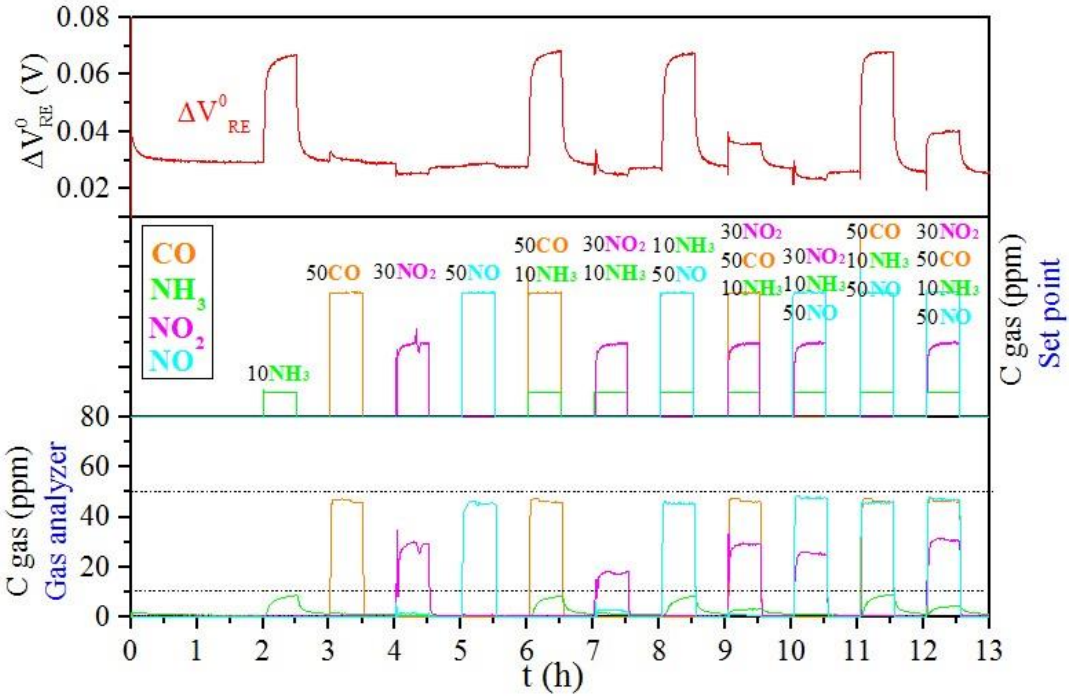

Fig. 7 Au-50% V_2O_5 sensor signal in a single gas or gas mixtures of CO, NH_3, NO_2, and NO at 550 °C with gas analysis at the cell exit.

For single gas, as expected, the sensor has high responses to 10 ppm of NH_3 (38 mV), no responses to 50 ppm CO and NO, and negligible negative responses to 30 ppm NO_2 at 550 °C. In binary gas mixtures, when injecting NH_3 in the presence of NO_2, it can be seen through gas analyzer that there is no more NH_3 gas at the exit. Furthermore, NO_2 concentration is slightly decreased (around 20 ppm) compared to the single gas measurement (around 30 ppm). In fact, this phenomenon is also observed when there is no sensor in the cell. This means that a reaction in gas phase occurs between NH_3 and NO_2, and NH_3 is completely consumed by NO_2 (according to reaction (1)) in our experimental conditions. Hence, the absence of sensor response to NH_3 when mixed with NO_2 is simply explained by the fact there is no more NH_3 in the gas phase, and it is also coherent with lower NO_2 concentration at the cell exit. Looking at the sensor response in other binary gas mixtures, CO and NO gases do not affect significantly sensor response to NH_3.

$$2NO_2 + O_2 + 4NH_3 \rightarrow 3N_2 + 6H_2O \qquad (1)$$

Considering the gas analyzer results in three-gas mixtures, the main results are similar to those observed in two gas mixtures. The sensor response to NH_3 is coherent with gas analyzer results. If NH_3 is consumed by NO_2, the sensor logically does not show significant responses. It is also

noticed that CO presence may limit NO_2/NH_3 reaction. Therefore, NH_3 is detected in NO_2/NH_3 gas mixtures only in the presence of CO. As a conclusion, the results show that the sensor responds to NH_3 whenever it is present in the gas phase, and sensor responses to other gases are negligible.

3.6 Sensitivity to NH_3 with varying oxygen concentrations

All previous tests were performed with a fixed oxygen content at 12 mol.%. In real conditions, its content can vary suddenly in a great range. Hence, sensing performances were studied at 550 °C by stepwise change in the NH_3 concentration from 2 to 40 ppm (2, 4, 8, 16, 32, and 40 ppm) at four different concentrations of oxygen (2%, 5%, 12%, and 16.4 mol.%). The results are shown in Fig. 8. It can be seen that the sensor baseline (when there is no NH_3), decreases with increasing O_2 concentration. The results also indicate that the sensor has a high sensitivity to ammonia, even at low concentrations (2 ppm), but it is influenced by the oxygen concentration. This phenomenon indicates competitive adsorption between NH_3 and O_2 on the sensing electrode, which is modeled in the next part.

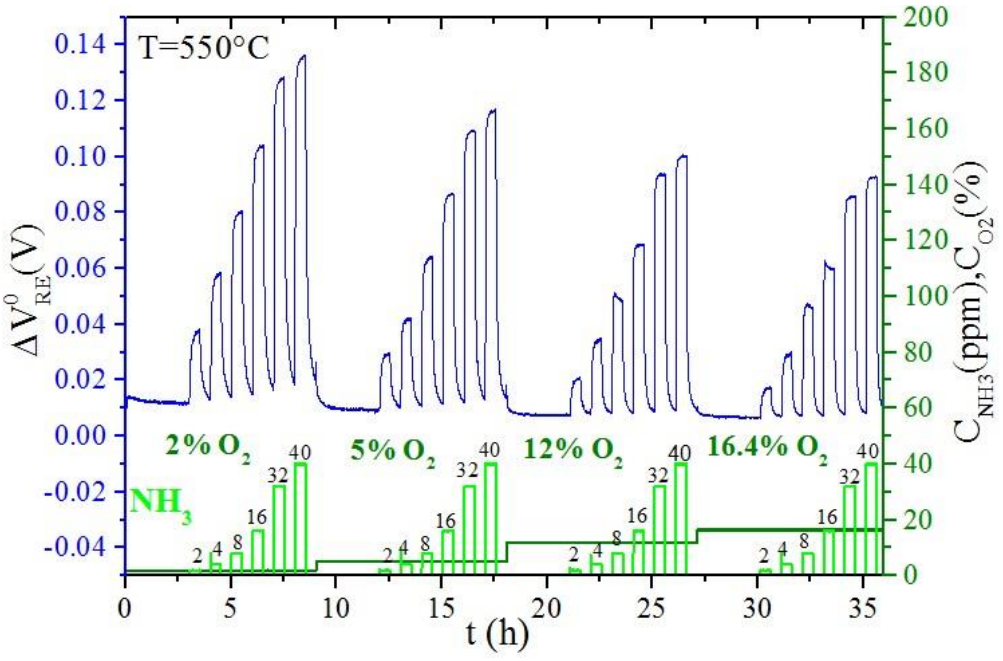

Fig. 8 Au-50%V_2O_5 sensors signal for different concentrations of NH_3 (2, 4, 8, 16, 32, and 40 ppm) at four oxygen concentrations (2, 5, 12, and 16.4 mol.%) at 550 °C.

Fig. 9 shows the variations of NH_3 signals as a function of log(C_{NH3}). It is seen that the signal changes linearly with the logarithm of NH_3 concentrations in the examined range. This is in agreement with reported results on planar potentiometric sensor [4, 24] and mixed potential theory [25, 26]. The slopes of the obtained lines indicate the sensitivity of the sensor to ammonia (defined with log(C_{NH3})), which are respectively 75.9, 69.2, 62.4, and 58.6 mV/decades for 2%, 5%, 12%, and 16.4% O_2 concentrations. Therefore, NH_3 sensitivity of the sensor decreases by increasing O_2 concentration. These values are in the same range as NH_3 potentiometric sensor reported in the literature [4, 24].

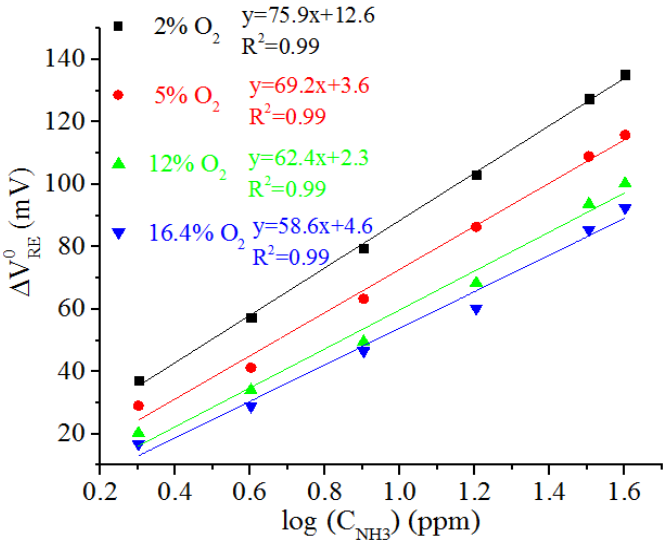

Fig. 9 Variations of Au-50%V_2O_5 sensor signals as a function of log(C_{NH3}) at 550 °C, for the four studied oxygen concentrations.

4. Modeling of NH_3 responses under different O_2 concentrations

Based on the previous experimental results (Fig. 8), and on the semi-logarithmic behavior of NH_3 responses plotted in Fig. 9, a model is proposed to quantify sensor responses. For this modeling, sensor responses in the base gas (considering only electrochemical oxygen reaction) and with NH_3 injections (mixed potential theory) are considered separately.

4.1 Baseline modeling (C_{NH3} = 0)

For the baseline of the sensor (when C_{NH3} = 0), an equilibrium condition is assumed for the unique electrochemical reaction of the oxygen (reaction 2, no mixed potential), so Nernst

equation is used for calculating the potential of each electrode and finally the electromotive force, which corresponds to the sensor signal ΔV_{RE}^{0} given by equation 3. In this relation, C_{O2}(RE) and C_{O2}(SE) should rigorously be the activity of adsorbed oxygen species at respectively the reference electrode (Pt) and sensing electrode (Au-V_2O_5) [27]. We made the hypothesis that the activity is equal to the concentrations of the considered species in the gas phase and more specifically the concentration in the gas phase at the three boundary points (electrode/YSZ/O_2 interface) of each electrode. Since platinum is a highly active catalyst for oxygen reduction (reaction 2), it is assumed that the oxygen concentration C_{O2}(RE) is equal to the oxygen concentration fixed in the gas phase. On the contrary, for the sensing Au-V_2O_5 electrode, due to the lower catalytic activity compared to platinum, the oxygen concentration at SE/YSZ/O_2 interface will be lower, resulting in varying sensor signals versus oxygen concentration in the base gas $\Delta V_{RE}^{0}\ (C_{NH3} = 0)$.

$$1/2O_2 + 2e^- \rightarrow O^{2-} \qquad (2)$$

$$\Delta V_{RE}^{0}\ (C_{NH3} = 0) = E_{O_2}(RE) - E_{O_2}(SE) = -\frac{RT}{4F} ln \frac{C_{O2}(SE)}{C_{O2}(RE)} \qquad (3)$$

Through Eq. 3 and experimental measurements of $\Delta V_{RE}^{0}\ (C_{NH3} = 0)$, $C_{O2}\ (SE)$ can be calculated and values are summarized in Table 2.

Table 2 Calculated oxygen concentrations on the sensing electrode at 550°C.

O_2 concentration in gas stream C_{O2}(RE) (mol.%)	$\Delta V_{RE}^{0}\ (C_{NH3} = 0)$ (V)	Calculated O_2 concentration on sensing electrode C_{O2} (SE) (mol.%)
2	0.012	1
5	0.009	3
12	0.008	7.7
16.4	0.007	11

4.2 NH_3 responses modeling

At the electrodes of a typical mixed-potential ammonia sensor [4, 28], the reduction reaction of oxygen (reaction 2) competes with the oxidation reaction of ammonia (reaction 4).

$$2/3\mathrm{NH_3} + \mathrm{O^{2-}} \rightarrow 1/3\mathrm{N_2} + 2\mathrm{e^-} + \mathrm{H_2O} \quad (4)$$

A mixed potential is established in steady-state condition when the rates of oxidation and reduction reactions are equal.

According to the mixed-potential theory, the reaction rate-limiting kinetics follow the Butler-Volmer equation, and at high over-potentials, the electric current densities (for electrochemical reactions 2 and 4) can be described by Tafel behavior with Eqs. 5 and 6 [10, 16, 29, 30].

$$i_{NH_3} = i^0_{NH_3} exp\left[\frac{2\alpha_1 F(E - E^{0'}_{NH_3})}{RT}\right] \quad (5)$$

$$i_{O_2} = i^0_{O_2} exp\left[\frac{-2\alpha_2 F(E - E^{0'}_{O_2})}{RT}\right] \quad (6)$$

where E is the potential produced by either NH_3 oxidation or O_2 reduction reactions, $i^0_{NH_3}$ and $i^0_{O_2}$ are the exchange current densities of NH_3 and O_2, $E^{0'}_{NH_3}$ and $E^{0'}_{O_2}$ are the standard potentials for NH_3 and O_2 reactions, α_1 and α_2 are the transfer coefficients of NH_3 and O_2, T is the temperature, F is the Faraday constant, and R is the gas ideal constant.

Supposing that the exchange current densities follow Freundlich isotherm, $i^0_{NH_3}$ and $i^0_{O_2}$ can be expressed by Eqs. 7 and 8 [10, 16, 29].

$$i^0_{NH_3} = B_1 C^n_{NH3} \quad (7)$$

$$i^0_{O_2} = -B_2 C^m_{O2} \quad (8)$$

Where B_1, B_2, m, and n are Freundlich constants, C_{NH3} and C_{O2} are concentrations of ammonia and oxygen respectively. When reactions 2 and 4 reach a dynamic balance ($i_{NH_3} + i_{O_2} = 0$), the mixed potential is established (Eq. 9).

$$E_{mix} = E_0 + mA^{"} lnC_{O2} - nA^{"} lnC_{NH3} \quad (9)$$

Where

$$E_0 = \frac{RT}{2(\alpha_1 + \alpha_2)F} ln \frac{B_2}{B_1} + \frac{\alpha_1 E_{NH_3}^{0'} + \alpha_2 E_{O_2}^{0'}}{\alpha_1 + \alpha_2} \quad (10)$$

$$A^{"} = \frac{RT}{2(\alpha_1 + \alpha_2)F} \quad (11)$$

As said before, assuming that the platinum electrode behaves like a "real" reference electrode, its mixed potential is close to 0 (E_{mix}(RE)~0) [21]. Consequently, according to Eq. 12, the signal of the sensor is equal to the negative of the mixed potential of the sensing electrode.

$$\Delta V_{RE}^0 \ (C_{NH3} \neq 0) = E_{mix}(RE) - E_{mix}(SE) \sim -E_{mix}(SE) \quad (12)$$

To calculate the mixed potential of the sensing electrode using Eqs. 9 to 11, estimated values of $\boldsymbol{E_{NH_3}^{0'}}$, $\boldsymbol{E_{O_2}^{0'}}$, B_1, B_2, m, and n parameters are derived from the literature [31-33]. These values are listed in Table 3.

Table 3 Parameter used for the sensor response modeling, issued from the literature [31-33].

Parameter	Value (unit)
$E_{O_2}^{0'}$	1.22 (V)
$E_{NH_3}^{0'}$	-0.77 (V)
m	0.5
n	0.885
B_2	0.0642
B_1	0.4227

Then, using the experimental results (ΔV_{RE}^0 as a function of C_{O2} and C_{NH3}), and optimizing α_1 and α_2 by means of a solver (Excel Solver, minimizing the sum of error squares), all values are determined and listed in Table 4. The obtained total mean square error is equal to 1.3×10^{-4}. From these calculated parameters, it is now possible to estimate the sensor signal for different NH_3 injections ($\Delta V_{RE}^0 \ (C_{NH3} \neq 0)$).

Table 4 Parameter values issued from experimental results fitting.

Parameter	Obtained value (unit)
α_1	0.92
α_2	0.32
E_0	-0.312 (V)
$A^{"}$	0.029

4.3 Integration of baseline and NH_3 responses modeling

Finally, the results of data modeling for the baseline (C_{NH3}=0), according to Nernst equation (equation 3) and for different concentrations of ammonia (C_{NH3} ≠0), according to mixed potential theory (equations 5 to 12), are plotted in Fig. 10 along with the experimental data. There is a good agreement between the model estimated from the previous calculations (orange curve) and experimental results (blue curve). Consequently, this validates the proposed model to describe ammonia response of the used single chamber sensor.

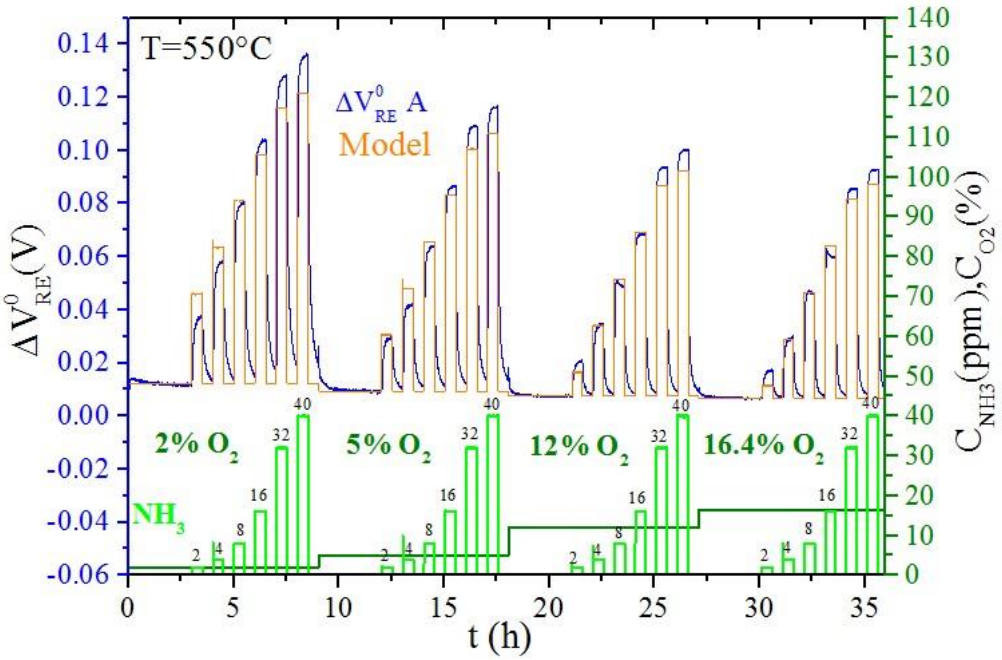

Fig. 10 Comparing modeling and experimental results for Au-50%V_2O_5 sensor to different concentration of NH_3 (2, 4, 8, 16, 32, and 40 ppm) and four concentrations of oxygen (2%, 5%, 12%, and 16.4%) at 550 °C.

Conclusion

For developing a selective mixed-potential ammonia sensor, a vanadium oxide-based material (Au-V_2O_5) was tested as sensing electrodes of a two-electrode structure sensor. The results showed that the selectivity of the sensor is dependent on the operating temperature and on the V_2O_5 content of the sensing electrode. By increasing V_2O_5 content in sensing electrode from 15 wt.% to 50 wt.%, selective ammonia sensors were achieved at 550 °C with high ammonia sensitivity around (62 mV/decades for 12 mol.% O_2 in the base gas). The sensors with Au-50wt.%V_2O_5 electrodes showed no cross-sensitivity to CO, NO_2, NO, H_2 and Hydrocarbons at 550 °C and also in gas mixtures of CO, NH_3, NO_2, and NO gases. The obtained responses from this sensor were modeled successfully according to Nernst and Butler-Volmer equations.

References

[1] L. Dai, G. Yang, H. Zhou, Z. He, Y. Li, L. Wang, Mixed potential NH_3 sensor based on Mg-doped lanthanum silicate oxyapatite, Sensors and Actuators B: Chemical. 224 (2016) 356–363. https://doi.org/10.1016/j.snb.2015.10.071.

[2] N. Miura, T. Sato, S.A. Anggraini, H. Ikeda, S. Zhuiykov, A review of mixed-potential type zirconia-based gas sensors, Ionics. 20 (2014) 901–925. https://doi.org/10.1007/s11581-014-1140-1.

[3] I. Lee, B. Jung, J. Park, C. Lee, J. Hwang, C.O. Park, Mixed potential NH_3 sensor with $LaCoO_3$ reference electrode, Sensors and Actuators B: Chemical. 176 (2013) 966–970. https://doi.org/10.1016/j.snb.2012.09.009.

[4] D. Schönauer-Kamin, M. Fleischer, R. Moos, Half-Cell Potential Analysis of an Ammonia Sensor with the Electrochemical Cell Au | YSZ | Au, V_2O_5-WO_3-TiO_2, Sensors. 13 (2013) 4760–4780. https://doi.org/10.3390/s130404760.

[5] L. -k. Tsui, A.D. Benavidez, P. Palanisamy, L. Evans, F.H. Garzon, A Three Electrode Mixed Potential Sensor for Gas Detection and Discrimination, ECS Transactions. 75 (2016) 9–22. https://doi.org/10.1149/07516.0009ecst.

[6] P. Pasierb, M. Rekas, Solid-state potentiometric gas sensors—current status and future trends, Journal of Solid State Electrochemistry. 13 (2009) 3–25. https://doi.org/10.1007/s10008-008-0556-9.

[7] V.V. Plashnitsa, P. Elumalai, Y. Fujio, N. Miura, Zirconia-based electrochemical gas sensors using nano-structured sensing materials aiming at detection of automotive exhausts, Electrochimica Acta. 54 (2009) 6099–6106. https://doi.org/10.1016/j.electacta.2008.12.040.

[8] W. Meng, L. Dai, W. Meng, H. Zhou, Y. Li, Z. He, L. Wang, Mixed-potential type NH_3 sensor based on TiO_2 sensing electrode with a phase transformation effect, Sensors and Actuators B: Chemical. 240 (2017) 962–970. https://doi.org/10.1016/j.snb.2016.09.021.

[9] D.Y. Wang, R.J. Robert, C.A. Valdes, E.M. Briggs, K.K. Polikarpus, J. Kupe, W.T. Symons, Ammonia gas sensors, US Patent 7,074,319, 2006.

[10] B. Wang, S. Yao, F. Liu, Y. Guan, X. Hao, X. Liang, F. Liu, P. Sun, Y. Wang, H. Song, G. Lu, Fabrication of well-ordered porous array mounted with gold nanoparticles and enhanced sensing properties for mixed potential-type zirconia-based NH_3 sensor, Sensors and Actuators B: Chemical. 243 (2017) 1083–1091. https://doi.org/10.1016/j.snb.2016.12.094.

[11] F. Liu, S. Li, J. He, J. Wang, R. You, Z. Yang, L. Zhao, P. Sun, X. Yan, X. Liang, X. Chuai, G. Lu, Highly selective and stable mixed-potential type gas sensor based on stabilized zirconia and $Cd_2V_2O_7$ sensing electrode for NH_3 detection, Sensors and Actuators B: Chemical. 279 (2019) 213–222. https://doi.org/10.1016/j.snb.2018.09.024.

[12] C. Wang, X. Li, F. Xia, H. Zhang, J. Xiao, Effect of V_2O_5-content on electrode catalytic layer morphology and mixed potential ammonia sensor performance, Sensors and Actuators B: Chemical. 223 (2016) 658–663. https://doi.org/10.1016/j.snb.2015.09.145.

[13] D. Schönauer, T. Nieder, K. Wiesner, M. Fleischer, R. Moos, Investigation of the electrode effects in mixed potential type ammonia exhaust gas sensors, Solid State Ionics. 192 (2011) 38–41. https://doi.org/10.1016/j.ssi.2010.03.028.

[14] V.V. Plashnitsa, P. Elumalai, Y. Fujio, T. Kawaguchi, N. Miura, Spontaneous gradual accumulation of hexagonally-aligned nano-silica on gold nanoparticles embedded in stabilized zirconia: a pathway from catalytic to NH_3-sensing performance, Nanoscale. 3 (2011) 2286–2293. https://doi.org/10.1039/c1nr10091b.

[15] A. Satsuma, M. Katagiri, S. Kakimoto, S. Sugaya, K. Shimizu, Effects of Calcination Temperature and Acid-Base Properties on Mixed Potential Ammonia Sensors Modified by Metal Oxides, Sensors. 11 (2011) 2155–2165. https://doi.org/10.3390/s110202155.

[16] F. Liu, R. Sun, Y. Guan, X. Cheng, H. Zhang, Y. Guan, X. Liang, P. Sun, G. Lu, Mixed-potential type NH3 sensor based on stabilized zirconia and $Ni_3V_2O_8$ sensing electrode, Sensors and Actuators B: Chemical. 210 (2015) 795–802. https://doi.org/10.1016/j.snb.2015.01.043.

[17] V. Modafferi, S. Trocino, A. Donato, G. Panzera, G. Neri, Electrospun V_2O_5 composite fibers: Synthesis, characterization and ammonia sensing properties, Thin Solid Films. 548 (2013) 689–694. https://doi.org/10.1016/j.tsf.2013.03.137.

[18] A. Morata, J. Viricelle, A. Tarancon, G. Dezanneau, C. Pijolat, F. Peiro, J. Morante, Development and characterisation of a screen-printed mixed potential gas sensor, Sensors and Actuators B: Chemical. (2007) 561–566.

[19] J. Gao, J.-P. Viricelle, C. Pijolat, P. Breuil, P. Vernoux, A. Boreave, A. Giroir-Fendler, Improvement of the NOx selectivity for a planar YSZ sensor, Sensors and Actuators B: Chemical. 154 (2011) 106–110. https://doi.org/10.1016/j.snb.2010.01.033.

[20] I. Romanytsia, J.-P. Viricelle, P. Vernoux, C. Pijolat, Application of advanced morphology Au–X (X=YSZ, ZrO_2) composites as sensing electrode for solid state mixed-potential exhaust NO_x sensor, Sensors and Actuators B: Chemical. 207 (2015) 391–397. https://doi.org/10.1016/j.snb.2014.10.017.

[21] N. Miura, T. Raisen, G. Lu, N. Yamazoe, Highly selective CO sensor using stabilized zirconia and a couple of oxide electrodes, Sensors and Actuators B: Chemical. 47 (1998) 84–91. https://doi.org/10.1016/S0925-4005(98)00053-7.

[22] R. Levi, M. Bar-Sadan, A. Albu-Yaron, R. Popovitz-Biro, L. Houben, Y. Prior, R. Tenne, Stability Criteria of Fullerene-like Nanoparticles: Comparing V_2O_5 to Layered Metal Dichalcogenides and Dihalides, Materials. 3 (2010) 4428–4445. https://doi.org/10.3390/ma3084428.

[23] K. Gupta, Effect of Post Annealing on the Structural Properties of Vanadium Oxide Thin Film Deposited by RF Sputtering, Indian Journal of Science and Technology. 10 (2017) 1–5. https://doi.org/10.17485/ijst/2017/v10i42/115790.

[24] D. Schönauer, K. Wiesner, M. Fleischer, R. Moos, Selective mixed potential ammonia exhaust gas sensor, Sensors and Actuators B: Chemical. 140 (2009) 585–590. https://doi.org/10.1016/j.snb.2009.04.064.

[25] J.W. Fergus, Sensing mechanism of non-equilibrium solid-electrolyte-based chemical sensors, Journal of Solid State Electrochemistry. 15 (2011) 971–984. https://doi.org/10.1007/s10008-010-1046-4.

[26] E. Comini, G. Faglia, G. Sberveglieri, eds., Solid state gas sensing, Springer, New York, NY, 2009.

[27] C.O. Park , N. Miura, Absolute potential analysis of the mixed potential occurring at the oxide/YSZ electrode at high temperature in NOx-containing air, Sensors and Actuators B: Chemical. B 113 (2006) 316–319. https://doi.org/10.1016/j.snb.2005.03.010.

[28] R. Moos, J. Kita, Ceramic multilayer gas sensors-An overview, in: XXXI International Conference of IMAPS Poland Chapter, Rzeszów-Krasiczyn, 2007.

[29] F. Garzon, Solid-state mixed potential gas sensors: theory, experiments and challenges, Solid State Ionics. 136–137 (2000) 633–638. https://doi.org/10.1016/S0167-2738(00)00348-9.

[30] T. Ritter, J. Lattus, G. Hagen, R. Moos, On the influence of the NOx equilibrium reaction on mixed potential sensor signals: A comparison between FE modelling and experimental data, Sensors and Actuators B: Chemical, 296 (2019) 126627. https://doi.org/10.1016/j.snb.2019.12662

[31] A.A. Halim, H.A. Aziz, M.A.M. Johari, K.S. Ariffin, M.J.K. Bashir, Semi-Aerobic Landfill Leachate Treatment Using Carbon–Minerals Composite Adsorbent, Environmental Engineering Science. 29 (2012) 306–312. https://doi.org/10.1089/ees.2010.0204.

[32] H. Zhang, Y. Wang, Z. Wu, D.Y.C. Leung, An ammonia electrolytic cell with NiCu/C as anode catalyst for hydrogen production, Energy Procedia. 142 (2017) 1539–1544. https://doi.org/10.1016/j.egypro.2017.12.605.

[33] P. Vanýsek, Handbook of Chemistry and Physics, 88th ed., 2007.